RSC Advances

ROYAL SOCIETY OF CHEMISTRY

www.rsc.org/advances

Deprotonation Routes of Anthocyanidins in Aqueous Solution, pK_a Values, and Speciation under Physiological Conditions†

Jorge Rafael León-Carmona,[1] Annia Galano*[2,] Juan Raúl Alvarez-Idaboy,[1*]

[1]*Facultad de Química, Departamento de Física y Química Teórica, Universidad Nacional Autónoma de México, México DF 04510, México.*

[2] *Departamento de Química, Universidad Autónoma Metropolitana-Iztapalapa. San Rafael Atlixco 186, Col. Vicentina. Iztapalapa. C. P. 09340. México D. F. México*

Abstract

Anthocyanidins are water-soluble flavonoids that have numerous beneficial effects to human, and animal, health. At the same time, they present multiple acid-base equilibria that under physiological conditions may lead to a rather wide distribution of species. This particular feature might influence the activity and mechanism of action of anthocyanidins in living systems, depending on the *p*H of the environment. Therefore, a detailed knowledge of the acid-base behavior of these compounds is crucial to fully understand their ways of action. In this work, theoretical calculations within the frame of the Density Functional Theory (DFT) were carried out to investigate several aspects or those equilibria for 12 anthocyanidins. Their most likely deprotonation routes were elucidated, and most of their pK_a values are reported here for the first time. Their reliability was confirmed by comparison with the available experimental data, which led to a mean unsigned error of 0.31. The obtained pK_a values allowed to estimate the populations of the different species depending on the *p*H, and particular attention was paid to *p*H=7.4. Hopefully, the data provided here may contribute to gain better understanding on the complex processes involving anthocyanidins, under physiological conditions.

Keywords: order of deprotonation; acid constants; molar fractions; deprotonation energy; pK_a calculations.

† Experimental pK_a and calculated ΔG^0 values for the set of phenols used to obtain the k and C_0 parameters. Relative Gibbs energies of the possible deprotonation reactions. pK_a values of quercetin and kaempferol. Cartesian coordinates of the optimized geometries.

* To whom correspondence should be addressed. E-mail: agal@xanum.uam.mx, or jidaboy@unam.mx

Introduction

Anthocyanidins (Scheme 1) are water-soluble pigments that belong to the flavonoids family and constitute the aglycon counterparts of anthocyanins. Both, anthocyanins and anthocyanidins, are widely distributed in the plant kingdom, and are frequently responsible for the bright colors of fruits, flowers and vegetables. The most distinctive structural feature of this kind of flavonoids is the presence of a flavylium ion, while they mainly differ in the number and position of the OH groups. There are at least 23 naturally occurring anthocyanidins identified so far,[1] being cyanidin (Cyn), pelargonidin (Plg), peonidin (Pnd), delphinidin (Dlp), petunidin (Ptn) and malvidin (Mlv), the most common ones.

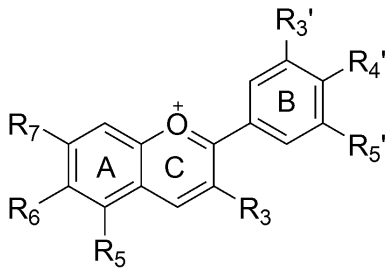

Scheme 1. General structure of anthocyanidins.

There is abundant evidence on the beneficial effects of anthocyanidins. For example, they have been found to be effective for protecting against the genotoxic damage induced by some chemotherapeutic drugs,[2] for preventing bone loss in post-menopausal osteoporosis,[3] and for inhibiting angiogenesis.[4] Anthocyanidins also offer protection against cardiovascular diseases,[5-8] light-induced retinal damage[9, 10] and ultraviolet induced DNA damage.[11] In addition, they also have anticarcinogenic[12, 13] and antioxidant[1, 14-16] effects.

At the same time, they present various hydroxyl groups in their structure, which are susceptible to deprotonation in aqueous solution, depending on the pH. The corresponding acid-dissociation constants (K_a) characterize the acidity of these compounds, which influence their chemical behavior. The K_a values –usually reported as pK_a– are related to numerous properties of drugs and nutrients, such as solubility and rate of absorption.[17] In addition, for compounds with more than one acid site, different deprotonation routes are possible. Let us use cyaniding ($R_3 = R_5 = R_7 = R_3' = R_4' = OH$) to illustrate this point. Formally it can have up to 5 acid-dissociation equilibria, i.e., up to 5 pK_a, one per each phenolic OH:

$$H_5Cyn^+ \underset{pKa1}{\overset{H^+}{\rightleftharpoons}} H_4Cyn \underset{pKa2}{\overset{H^+}{\rightleftharpoons}} H_3Cyn^- \underset{pKa3}{\overset{H^+}{\rightleftharpoons}} H_2Cyn^{2-} \underset{pKa4}{\overset{H^+}{\rightleftharpoons}} HCyn^{3-} \underset{pKa5}{\overset{H^+}{\rightleftharpoons}} Cyn^{4-}$$

However, while species H_5Cyn^+ and Cyn^{4-} are unambiguous, there are –in principle– 5, 10, 10, and 5 possible different species for H_4Cyn, H_3Cyn^-, H_2Cyn^{2-}, H_3Cyn^-, respectively, depending on which sites are deprotonated. Thus, elucidating which of them are the most likely ones becomes a crucial task in order to identify the dominant species at each *p*H of interest.

Such speciation may influence, at least, some of the beneficial effects attributed to polyphenols. For example, there are previous reports indicating that the chromatic properties[18] and antioxidant activity[19, 20] of these compounds may change depending on the dominant acid-base species. In the particular case of the antioxidant activity, this would affect not only the extension of the activity but also the main reaction mechanisms contributing to it. In addition, to our best knowledge the information gathered so far on the pK_a values of anthocyanidins is still limited (Table 1). It comprises the first pK_a values of 5 anthocyanidins that were experimentally obtained from absorption spectra, and the theoretical estimation of the second pK_a values for the same compounds. These estimations were made using a quantitative structure activity relationship that relates the experimental pK_a values of the OH groups in hydroxyflavones to the theoretically calculated deprotonation energies.[21]

Table 1. Previously reported pK_a values of anthocyanidins studied.[19]

Anthocyanidins	pK_{a1}[(a)]	pK_{a2}[(b)]
Cyanidin	5.48	6.39
Delphinidin	5.30	6.30
Malvinidin	6.02	7.40
Pelargonidin	5.79	7.05
Peonidin	5.93	7.37

[(a)] experimental values, [(b)] estimated using a quantitative structure activity relationship

Accordingly, the main goals of the present work are: (i) to identify the most like species for the first three deprotonations of a large series of anthocyanidins, and (ii) estimate their pK_{a1}, pK_{a2}, and pK_{a3} values. Subsequent deprotonations were not included in this investigation,

because they are assumed to be unimportant under physiological conditions. Thus, the results provided here are expected to contribute to a better characterization of the investigated compounds under such conditions, and hopefully to interpret their experimental behavior.

Computational Details

All the electronic calculations were performed with Gaussian 09 package of programs.[22] Geometry optimizations and frequency calculations have been carried out using the M05-2X functional[23] and the 6-311++G(d,p) basis set, in conjunction with the SMD continuum model[24] using water as solvent to mimic the aqueous environment. Local minima were identified by the absence of imaginary frequencies.

Deprotonation Routes

Thermodynamic corrections at 298.15 K were included in the calculation of relative energies, which have been computed for the 1 M standard state. To identify the most likely deprotonation routes, we started by investigating which first deprotonation has the lowest energy cost. Based on this information the most likely structure for H_4Cyn is proposed. Using this structure as a starting point, the second deprotonation is analyzed in a similar manner to identify H_3Cyn^-, and from this species the third deprotonation is investigated. This strategy allowed to reduce the number of possible structures. For example, for H_3Cyn^- and H_2Cyn^{2-} instead of 10 there are 4 and 3, respectively. Computational protocols have been previously used to successfully elucidate deprotonation routes of chemical compounds with multiple acid sites.[25-30]

*p*K$_a$ *Calculations*

Three *p*K$_a$ calculation strategies were evaluated in the present work, using the available experimental data (Table 1) as reference values. The first one is the isodesmic method, also known as the proton exchange method, or the relative method.[31] It is based on the following reaction scheme:

$$HA + Ref^- \rightleftharpoons A^- + HRef$$

with *HRef*/*Ref*$^-$ being an acid/base pair of a reference compound. Then the *p*K$_a$ can be calculated as:

$$pKa(HA) = \frac{\Delta G_s}{RT\ln(10)} + pKa(HRef) \quad (1)$$

The isodesmic method has been previously recommended to predict reliable pK_a values for phenolic deprotonations of relative large systems,[32] and has been successfully used to that purpose.[33, 34] It has been effective not only for estimating pK_as of pure organic molecules, but also for metal containing systems.[35] Further details on pK_a calculations using the isodesmic method, and continuum model solvents, can be found elsewhere.[36, 37]

The second strategy for calculating the anthocyanidins pK_a was the direct scheme:

$$HA \rightleftharpoons A^- + H^+$$

This was done because it is the most frequently used, probably due to its simplicity. One of the disadvantage of this scheme is that it involves the proton. It is known that computational methods poorly reproduce the solvation energies of this particular species. Therefore, the $\Delta G_g(H^+)$ and $\Delta G_{solv}(H^+)$ values used to calculate the Gibbs free energy of the deprotonation reactions are derived from experiments. However, the variations on the reported experimental values of the solvation free energy of the proton are rather large, with values ranging from -259 to -266 kcal/mol.[36] Such a variation is an important source of error in the calculated pK_as, i.e it alone represents about 3 pK_a units. In this work we have used $\Delta G_g(H^+)$= –4.39 kcal/mol and $\Delta G_{solv}(H^+)$= –265.89 kcal/mol, based on the recommendation of Camaioni and Schwerdtfeger.[38] In this case the pK_a is calculated as:

$$pKa(HA) = \frac{\Delta G_s}{RT\ln(10)} \quad (2)$$

The third strategy was previously proposed to avoid using the experimental data of the proton.[39, 40] Here it is referred to as the parameters fitting method. It consist of using the experimental pK_a values of a set of small reference molecules to obtain two empirical parameters (k and C_0) by fitting the following linear equation, that is derived from equation (2):

$$pKa_{\exp} = k\Delta G_{BA} + C_0 \quad (3)$$

where ΔG_{BA} is the difference in Gibbs energy between the conjugated base and the corresponding acid ($G_{calc(A-)} - G_{calc(HA)}$), calculated at the same level of theory than the investigated molecules, here M05-2X/6-311++G(d,p) and SMD (solvent=water). The reference set is chosen based on the kind of acid chemical group involved, in our case phenols (Table 1S, Electronic Supplementary Information, ESI). After obtaining parameters k and C_0, they are used to calculate the pK_a of the molecule of interest. Their values in this work are k = 0.298 and C_0 = –76.22, with R^2=0.973. Similar strategies have been successfully used to estimate pK_a values of other compounds,[28, 41-45] and

After identify the calculation strategy in best agreement with the experimental data, it was used to estimate the pK_a values of the studied anthocyanidins that have not been previously reported.

Results and discussion

The structural features of the 12 anthocyanidins studied in this work are shown in Table 2. In addition to the six most frequently found in nature, another six were also considered includign some methoxylated anthocyanidins and two 6-hydroxylated anthocyanidins. The molecules in the set differ not only in the number of phenolic OH, but also on the hydroxylated sites. This variety is expected to allow a detailed analysis on the influence of structural features on the acidity and deprotonation order of anthocyanidins.

Table 2. Anthocyanidins studied in this work, for all of them R_4'=OH. The site labels corresponds to those shown in Scheme 1.

Anthocyanidin	Acronym	R_3'	R_5'	R_3	R_5	R_6	R_7
Aurantinidin	Arn	H	H	OH	OH	OH	OH
Capensinidin	Cpn	OH	OCH_3	OH	OCH_3	H	OCH_3
Cyanidin	Cyn	OH	H	OH	OH	H	OH
Delphinidin	Dlp	OH	OH	OH	OH	H	OH
Europinidin	Erp	OCH_3	OH	OH	OCH_3	H	OH
Luteolinidin	Ltl	OH	H	H	OH	H	OH
Malvidin	Mlv	OCH_3	OCH_3	OH	OH	H	OH
Pelargonidin	Plg	H	H	OH	OH	H	OH
Peonidin	Pnd	OCH_3	H	OH	OH	H	OH

Petunidin	Ptn	OH	OCH_3	OH	OH	H	OH
Rosinidin	Rsn	OCH_3	H	OH	OH	H	OCH_3
6OH-Delphinidin	6Dlp	OH	OH	OH	OH	OH	OH

Deprotonation Routes

Different deprotonation steps, up to three, were included in this study for the studied anthocyanidins since they all have at least 3 acid sites. The acid dissociation equilibria were analyzed in the same order that they would follow in actual systems, as the *p*H increases. All the hydroxyl groups, at each deprotonation degree, were considered as potential acid sites. The relative Gibbs energies for the first deprotonations are shown in Table 2S, ESI. To facilitate comparisons the lowest energy for each anthocyanidin was set to zero and the other values in the table are reported with respect to them. It was found that the first deprotonation can involve rings A or B, depending on the particular anthocyanidin and the groups in each ring. The most acidic site is R_4' for Cyn, Dlp, Erp, Ltl, and Rsn; R_5 for Mlv and Ptn; and R_7 for Arn, Cpn, Plg, Pnd and 6Dlp. In general, within each anthocyanidin, the larger the number of OH groups next to an acid site, the easier the deprotonation from that site. In addition, analyzing compound 6Dlp –which presents pyrogallol-like structures in rings A and B– it seems that when similar groups are in the vicinity of the acid sites, deprotonation from ring A requires lower energy, albeit the difference is small.

The relative energies corresponding to the subsequent second and third deprotonation are provided in Tables 3S and 4S (ESI), respectively. For those anthocyanidins with the first deprotonation taking place from ring A the second one is most likely to involve ring B, while for those anthocyanidins first deprotonated place from ring B the second one takes place from rings A or C. For both, the second and the third deprotonation, a common feature is that the most likely deprotonation site is never next to a site already deprotonated in a previous acid-base equilibria.

For the three investigated acid-base equilibria there are some cases for which the relative deprotonation energies associated with more than one acid site are lower than 1 kcal/mol. Accordingly, in addition to the main deprotonation product, other species might be present to a non-negligible extent. The percent population, per site, of each possible conjugated base

yield by the 3 first deprotonation reactions of each investigated anthocyanidin (H_4A, H_3A^- and H_2A^{2-} for the first, second, and third deprotonation respectively) was estimated using the Maxwell-Boltzmann distribution (Figure 1).

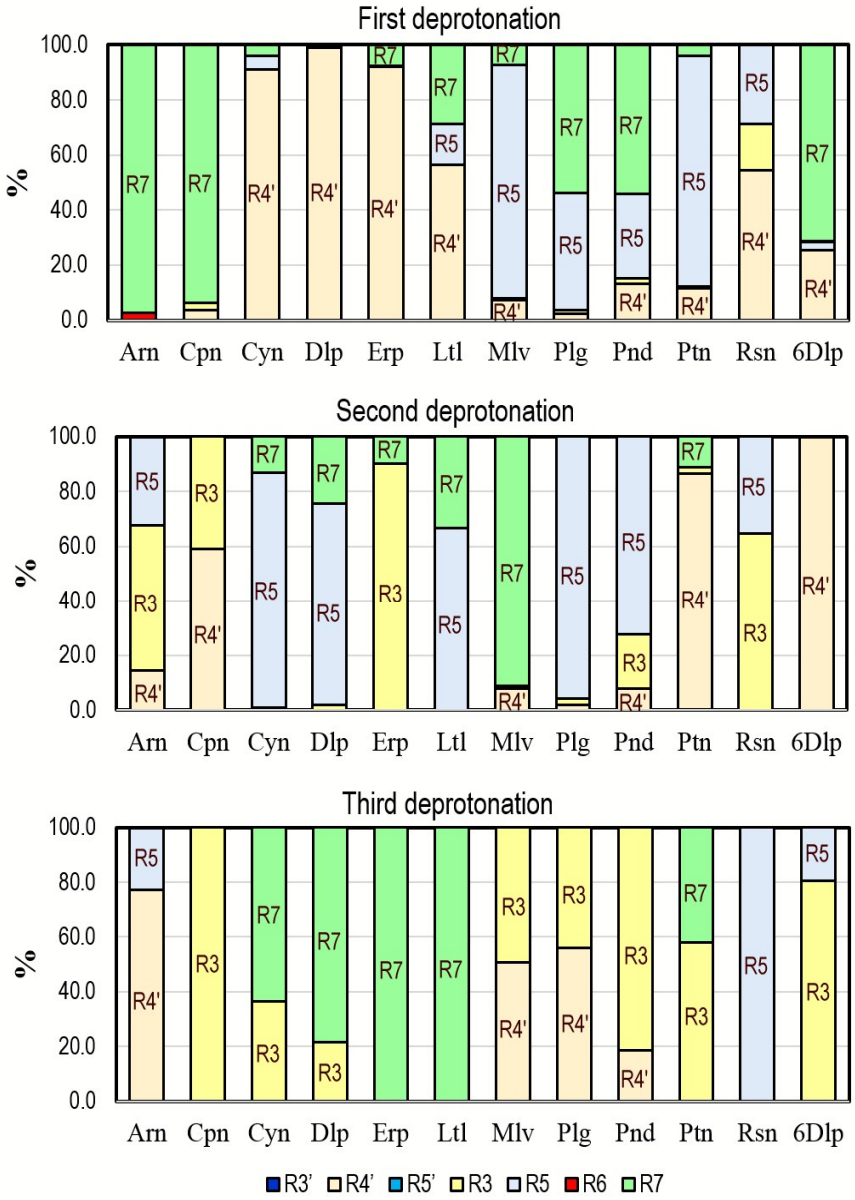

Figure 1. Percent population, per site, of the deprotonated forms (H_4A for the first deprotonation, H_3A^- for the second deprotonation, and H_2A^{2-} for the third deprotonation).

The first deprotonation yield mainly one conjugated base for Arn,Cpn, Cyn, Dlp, Erp, Mlv and Ptn, while more than one H_4A may be present in significant amounts for Ltl, Plg, Pnd, Rsn and 6Dlp. For the second deprotonation Cyn, Erp, Mlv, Plg, Ptn and 6Dlp yield mainly

one H_3A^-, while Arn, Cpn, Dlp, Ltl, Pnd and Psn tautomeric equilibria involving more than one conjugated base are expected. The third deprotonations yielding mainly one product are those involving Cpn, Erp, Ltl and Rsn; while for Arn, Cyn, Dlp, Mlv, Plg, Pnd, Ptn, and 6Dlp more than one H_2A^{2-} may coexist. Therefore the deprotonation routes (Schemes 2 and 3) proposed here correspond to the main pathways, but it should be kept in mind that other routes might also contribute –to a minor extent– to the acid base equilibria of the studied anthocyanidins.

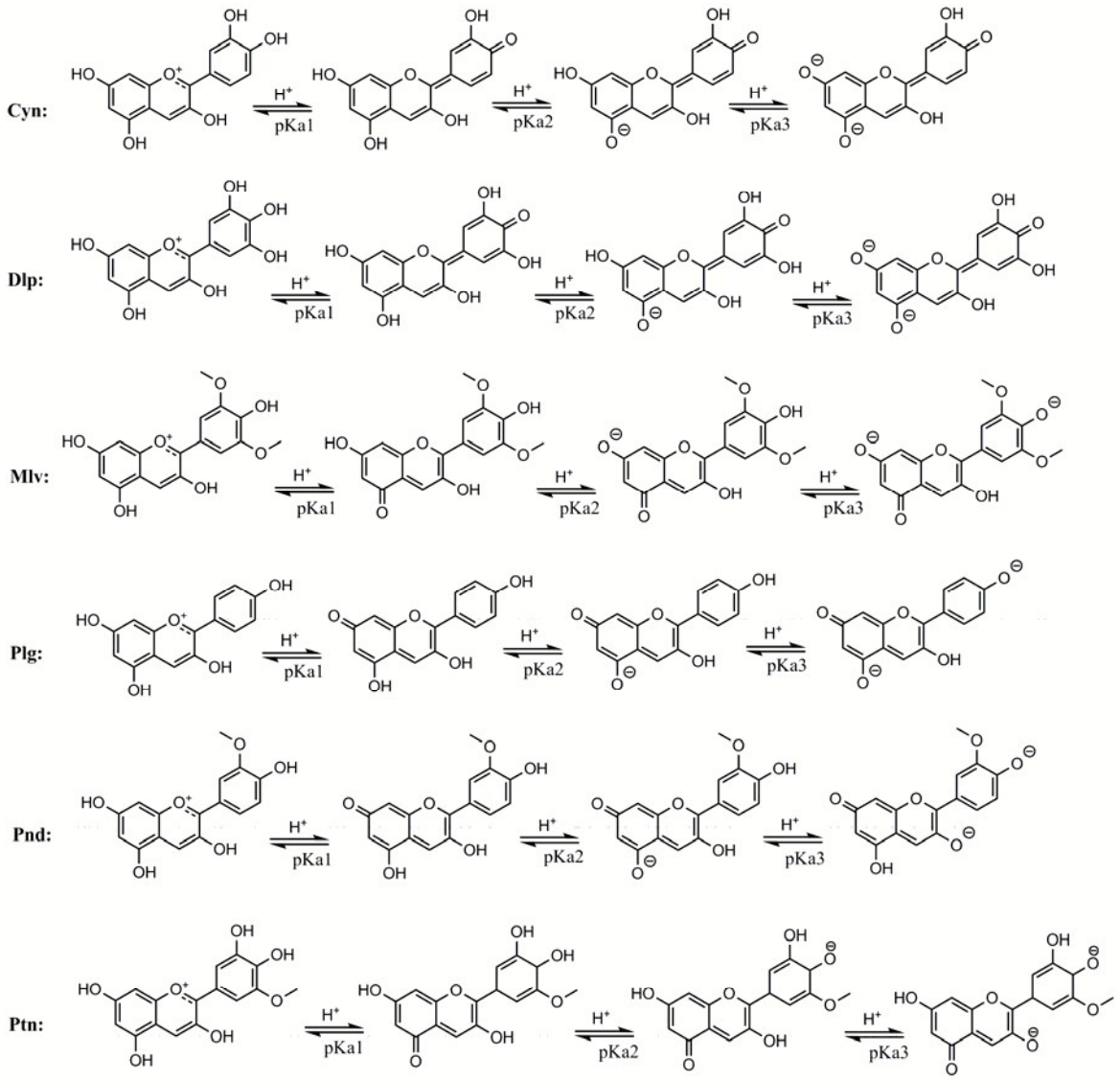

Scheme 2. Main deprotonation routes for the studied anthocyanidins most frequently found in nature.

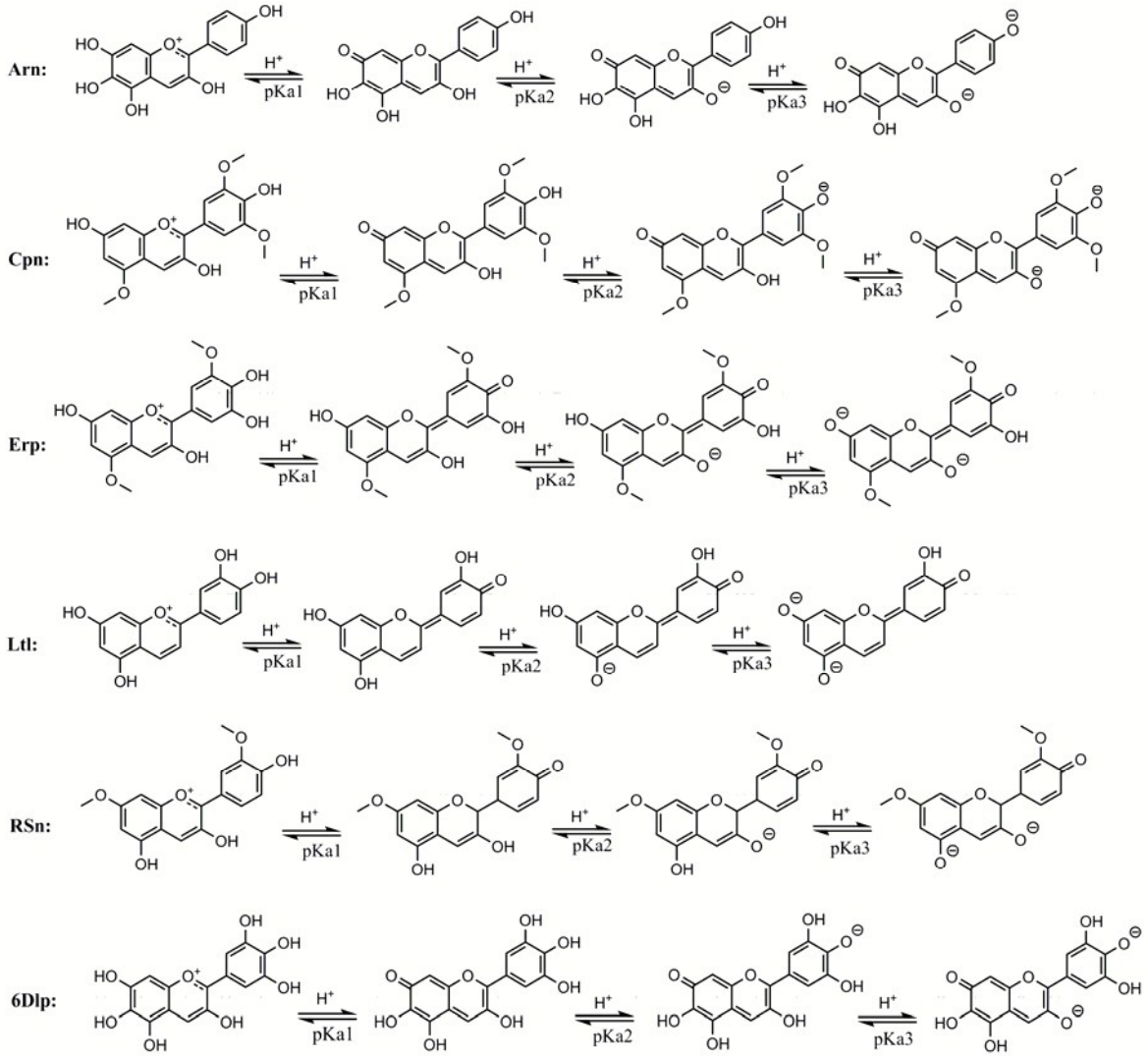

Scheme 3. Main deprotonation routes for the studied anthocyanidins that are not among the most frequently found in nature.

*p*K*a Calculations*

For the anthocyanidins investigated in this work, there are only 5 experimental pK_a values previously reported (Table 1). They have been used to assess the accuracy of three calculating strategies, namely (i) the isodesmic method, (ii) the direct method, and (iii) the fitting parameters method. The pK_a values calculated using these methods are reported in Table 3. For the isodesmic method to be reliable there are two key factors to keep in mind. *HRef*

should be structurally similar to the system of interest, and its experimental pK_a should be known. Therefore Cyn has been chosen as *HRef* here.

Table 3. Calculated pK_a values using the isodesmic (i), direct (ii) and fitting parameters (iii) methods for anthocyanidins with known experimental pK_{a1} values.

	Calc.(i)	Calc.(ii)	Calc.(iii)
Cyn		4.74	5.28
Dlp	6.23	4.10	4.97
Mlv	5.70	4.59	5.19
Plg	4.22	5.82	5.78
Pnd	4.36	5.70	5.73

The mean unsigned errors (MUE) and the maximum absolute error (MAE) obtained with the used strategies are shown in Figure 2. The best agreement with the experimental data was found for the fitting parameters method (iii), with MUE=0.31 and MAE=0.83 pK_a units, which are significantly lower than those obtained for the direct (MUE=0.73, MAE=1.43) and the isodesmic strategies (MUE=1.10, MAE=1.57). The performance of the fitting parameters method (using SMD, this work) is consistent with that previously found for other charged acids when using PCM and the Pauling cavity.[45] It should be noted, though, that UFF and UAKS cavities were reported to lead to larger errors.

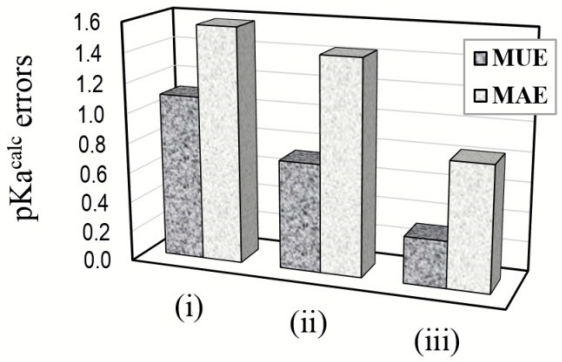

Figure 2. Mean unsigned errors (MUE) and maximum absolute errors (MAE) for the three tested pK_a calculation strategies, i.e., isodesmic (i), direct (ii) and fitting parameters (iii).

According to the above discussed results, the fitting parameters method has been chosen to estimate the first pK_a values of the rest of the investigated anthocyanidins, as well as for the

calculation of the second and third pK_a values of the whole set. In addition, it seems important to call attention to the fact that pK_a calculations still represent a challenging task. In fact, it has been proposed that methodologies yielding MUE~2 are considered reasonably accurate.[36] Thus, the agreement with the experimental data obtained here, when using the fitting parameters method, is actually very good.

However, since the validation of this method was tested only for first pK_as, because they are the only ones already estimated using experimental techniques for anthocyanidins, an additional test was performed. It consisted on testing the reliability of the fitting parameters method for other polyphenols (quercetin and kaempferol) for which there is experimental data available on their first, second and third pK_as. In fact, there are several values of pK_{a1}, pK_{a2} and pK_{a3} previously reported for these compounds, thus here we use the average values as references (Table 5S, ESI).

It is important to note that regarding the charge of the acid-base species pK_{a1} and pK_{a2} of quercetin and kaempferol are the most similar ones to pK_{a2} and pK_{a3} of anthocyanidins, i.e, in the first case the acid is neutral and the conjugated base is mono-anionic, and in the second case the acid is mono-anionic and the conjugated base is di-anionic. The agreement of the data calculated with the fitting parameters method from the experimental values of quercetin and kaempferol –considering pK_{a1}, pK_{a2}, and pK_{a3} altogether– was found to be good with MUE=0.54 and MAE=0.85. Therefore, it is expected that the fitting parameters method would be reliable for predicted not only the first pK_{as} of anthocyanidins but also the second and the third ones. In addition, the values of the second pK_a*s* calculated here are in good agreement with those previously estimated using a quantitative structure activity relationship.[19]

The values of pK_{a1}, pK_{a2} and pK_{a3} proposed here, using the fitting parameters method, for the whole set of investigated anthocyanidins are reported in Table 4. The first pK_a ranges from 4.75 to 6.19, with the lowest value corresponding to Arn and the largest to Rsn. The acidity, corresponding to the first deprotonation, decreases in the following order: Arn, 6Dlp, Dlp, Mlv, Cyn, Ptn, Cpn, Erp, Ltl, Pnd, Plg, Rsn. The three first present the pyrogallol moiety, which seems to increase the acidity of the investigated compounds, especially when it is in the A ring. In general, the larger the number of OH groups, and the lower the number of

OCH_3 substituents, the most acid the compound. In addition, the presence of an OH group at site R_3 decreases the acidity of the anthocyanidins that first deprotonate from ring A.

The second pK_a for the set of investigated anthocyanidins ranges from 6.27 (Dlp) to 7.83 (Arn ≈ Cpn), while the third one ranges from 7.88 (Rsn) to 8.91 (Plg). The second pK_a increases according to 6Dlp, Dlp, Cyn, Ltl, Ptn, Plg, Mlv, Erp, Pnd, Rsn, Cpn, Arn. Again the molecule that after the first deprotonation still has the pyrogallol moiety is the one that deprotonates the easiest in the second acid-base equilibria. For the third pK_a, the acidity in decreasing order is: Rsn, Dlp, 6Dlp, Ptn, Ltl, Cpn, Erp, Pnd, Arn, Cyn, Mlv, Plg.

Table 4. Proposed pK_{a1}, pK_{a2} and pK_{a3} values for the studied anthocyanidins.

	pK_{a1}	pK_{a2}	pK_{a3}
Arn	4.75	7.83	8.59
Cpn	5.50	7.83	8.40
Cyn	5.28	6.91	8.67
Dlp	4.97	6.81	8.08
Erp	5.64	7.35	8.44
Ltl	5.69	6.92	8.31
Mlv	5.19	7.26	8.73
Plg	5.79	7.20	8.91
Pnd	5.73	7.53	8.51
Ptn	5.38	6.99	8.27
Rsn	6.19	7.74	7.88
6Dlp	4.89	6.27	8.11

Using the pK_a values estimated here, the distribution diagrams of the investigated anthocyanidins were constructed in the 0 to 14 interval of *p*H (Figure 3). The values of the molar fractions at physiological *p*H (*p*H=7.4) are reported in Table 5, since this *p*H is particularly important in biological systems. Protonated anthocyanidins (H_5A^+) are only the dominant species at acid *p*Hs. However, their molar fractions rapidly decreases at *p*H ≥ 4, thus their biological importance in most of the human body regions, with the exception of the stomach, is expected to be negligible. The most deprotonated species considered in this

work (H_2A^{2-}) are only the main ones at basic *p*Hs (higher than 8.5-9.0), but contrary to H_5A^+ they can be present to a non-negligible extent at *p*Hs significant for biological processes.

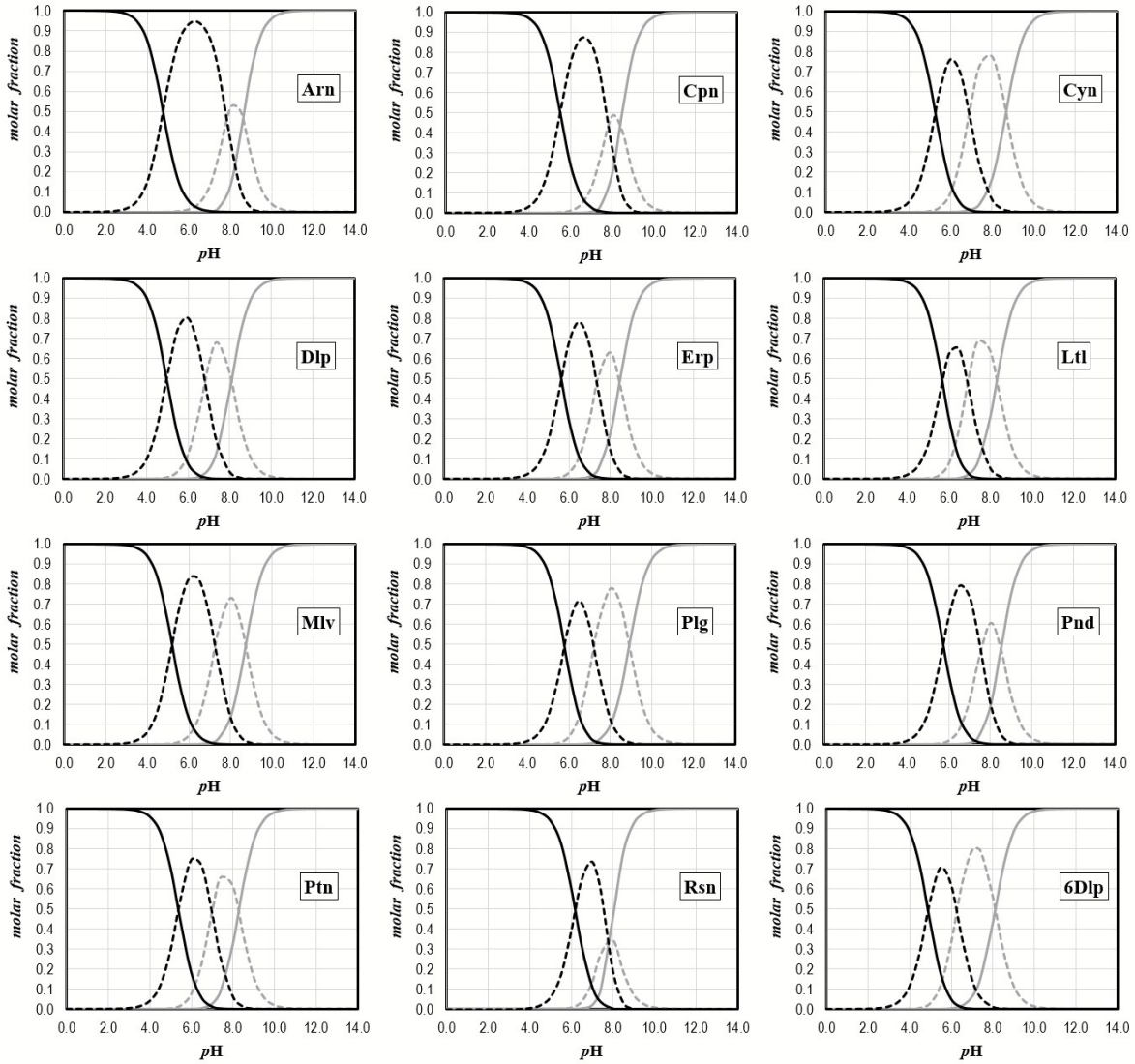

Figure 3. Distribution diagrams of the investigated anthocyanidins, including the species H_5A^+ (solid black lines), H_4A (dotted black lines), H_3A^- (dotted gray lines), and H_2A^{2-} (solid gray lines).

At *p*H values in the vicinity of the physiological one, there is more than one acid-base species with significant population for all the investigated anthocyanidins. The most significant cases in this context are Mlv and Pnd for which it is expected that H_4A and H_3A^- would be present in similar amounts at *p*H=7.4. For Cyn, Dlp, Ltl, Plg, Ptn and 6Dlp the main species is

predicted to be H_3A^- with populations ranging from 60 to 80%; while for Arn, Cpn and Rsn H_4A is the most abundant one. The dianion (H_2A^{2-}) is predicted to be in amounts larger than 5%, at this *p*H, for Dlp, Ltl, Ptn, Rsn and 6Dlp.

In addition, it should be pointed out that sometimes species existing in rather low molar fractions are responsible for the certain biological activities. One example is the free radical scavenging activity of resveratrol and piceatannol.[33] This is a dramatic example where albeit the molar fraction of anionic resveratrol is as low as 0.017 at physiological *p*H, it is still responsible for almost the whole protection against peroxyl radicals exerted by this antioxidant in water solution at this *p*H. In the case of the anthocyanidins investigated here, the lowest molar fraction found is also 0.017 (Table 5). Accordingly, the possible role of the H_2A^{2-} species in biological processes, such as the antioxidant protection, cannot be ruled out just yet.

Table 5. Molar fractions of H_5A^+, H_4A, H_3A^-, and H_2A^{2-} at physiological *p*H (*p*H=7.4) for the whole set of investigated anthocyanidins.

	H_2A^{2-}	H_3A^-	H_4A	H_5A^+
Arn	0.017	0.266	0.715	0.002
Cpn	0.026	0.262	0.702	0.009
Cyn	0.039	0.726	0.233	0.002
Dlp	0.142	0.682	0.175	0.001
Erp	0.046	0.500	0.447	0.008
Ltl	0.084	0.687	0.225	0.004
Mlv	0.026	0.561	0.410	0.003
Plg	0.018	0.595	0.377	0.009
Pnd	0.032	0.406	0.550	0.012
Ptn	0.089	0.655	0.254	0.002
Rsn	0.091	0.272	0.600	0.037
6Dlp	0.153	0.789	0.058	0.000

The estimated values of the molar fractions indicate that several acid base species should be considered regarding the potential biological roles of anthocyanidins. Moreover, the rather wide distribution of acid-base species predicted for this family of compounds suggests that

their mechanism of action, for example as antioxidants, should be complex and influenced by the *p*H of the environment. It is expected that the data provided here for the first time help interpreting the experimental behavior of anthocyanidins under conditions similar to those relevant to biological systems.

Conclusions

The 3 first acid-base equilibria of 12 anthocyanidins were investigated using theoretical calculations within the frame of the Density Functional Theory (DFT). Their most likely deprotonation routes were elucidated, and proposed here for the first time.

Three computational methodologies for predicting pK_a values were tested using the available experimental data as reference. They are the isodesmic method, the direct method and the fitting parameters method. The latter was found to be the one leading to the best agreement with the experiments, with MUE=0.31 and MAE=0.83 pK_a units. Therefore, it was chosen to calculate the whole set of pK_a values.

pK_{a1}, pK_{a2} and pK_{a3} were calculated for the investigated anthocyanidins and used to estimate their molar fractions in the 0 to 14 *p*H range. It was found that at physiological *p*H more than one acid base species are present to a significant extent for all the studied molecules. The population of H_5A^+ is proposed to be negligible at this *p*H, while the most abundant species are expected to be H_4A and H_3A^-. However, due to the usual higher reactivity of more deprotonated species in some biological activities, such as the antioxidant protection, H_2A^{2-} cannot be neglected.

Hopefully, the data provided here may contribute to gain better understanding on the complex processes involving anthocyanidins, under physiological conditions.

Acknowledgements

This work was carried out using a NES supercomputer, provided by Dirección General de Cómputo y Tecnologías de Información y Comunicación (DGTIC). This work was partially supported by projects SEP-CONACyT 167491 and 167430, and DGAPA PAPIIT-

IN220215. J.R.L.-C. acknowledges the financial support to CONACyT in the form of postdoctoral fellowship.

References

1. H. M. Ali, W. Almagribi and M. N. Al-Rashidi, *Food Chemistry*, 2016, **194**, 1275-1282.
2. N. Khandelwal and S. K. Abraham, *Planta Medica*, 2014, **80**, 1278-1283.
3. S. Moriwaki, K. Suzuki, M. Muramatsu, A. Nomura, F. Inoue, T. Into, Y. Yoshiko and S. Niida, *PLoS ONE*, 2014, **9**.
4. N. Matsunaga, K. Tsuruma, M. Shimazawa, S. Yokota and H. Hara, *Phytotherapy Research*, 2010, **24**, S42-S47.
5. H. M. Hügel, N. Jackson, B. May, A. L. Zhang and C. C. Xue, *Phytomedicine*, 2016, **23**, 220-231.
6. M. J. Kruger, N. Davies, K. H. Myburgh and S. Lecour, *Food Research International*, 2014, **59**, 41-52.
7. T. C. Wallace, *Advances in nutrition (Bethesda, Md.)*, 2011, **2**, 1-7.
8. P. J. Mink, C. G. Scrafford, L. M. Barraj, L. Harnack, C. P. Hong, J. A. Nettleton and D. R. Jacobs Jr, *American Journal of Clinical Nutrition*, 2007, **85**, 895-909.
9. H. Jia, W. Chen, X. Yu, X. Wu, S. Li, H. Liu, J. Liao, W. Liu, M. Mi, L. Liu and D. Cheng, *Journal of Veterinary Science*, 2013, **14**, 345-353.
10. J. Tanaka, T. Nakanishi, K. Ogawa, K. Tsuruma, M. Shimazawa, H. Shimoda and H. Hara, *Journal of Agricultural and Food Chemistry*, 2011, **59**, 528-536.
11. W. Liu, X. Lu, G. He, X. Gao, M. Li, J. Wu, Z. Li, J. Wu, J. Wang and C. Luo, *Biotechnology Letters*, 2013, **35**, 491-498.
12. H. Kausar, J. Jeyabalan, F. Aqil, D. Chabba, J. Sidana, I. P. Singh and R. C. Gupta, *Cancer Letters*, 2012, **325**, 54-62.
13. C. P. Hsu, Y. T. Shih, B. R. Lin, C. F. Chiu and C. C. Lin, *Journal of Agricultural and Food Chemistry*, 2012, **60**, 3686-3692.
14. H. S. Barcena, P. Chen and A. Tuachi, *SpringerPlus*, 2015, **4**.
15. R. A. Mosquera, L. Estévez and M. G. Bugarín, *Journal*, 2015, **1208**, 257-276.
16. J. Azevedo, I. Fernandes, A. Faria, J. Oliveira, A. Fernandes, V. d. Freitas and N. Mateus, *Food Chemistry*, 2010, **119**, 518-523.
17. T. N. Brown and N. Mora-Diez, *The Journal of Physical Chemistry B*, 2006, **110**, 9270-9279.
18. F. J. Heredia, E. M. Francia-Aricha, J. C. Rivas-Gonzalo, I. M. Vicario and C. Santos-Buelga, *Food Chemistry*, 1998, **63**, 491-498.
19. T. Borkowski, H. Szymusiak, A. Gliszczyńska-Świgło, I. M. C. M. Rietjens and B. Tyrakowska, *Journal of Agricultural and Food Chemistry*, 2005, **53**, 5526-5534.
20. L. Estévez, N. Otero and R. A. Mosquera, *Journal of Physical Chemistry B*, 2010, **114**, 9706-9712.
21. K. Lemańska, H. Szymusiak, B. Tyrakowska, R. Zieliński, A. E. M. F. Soffers and I. M. C. M. Rietjens, *Free Radical Biology and Medicine*, 2001, **31**, 869-881.

22. M. J. Frisch, G. W. Trucks, H. B. Schlegel, G. E. Scuseria, M. A. Robb, J. R. Cheeseman, G. Scalmani, V. Barone, B. Mennucci, G. A. Petersson, H. Nakatsuji, M. Caricato, X. Li, H. P. Hratchian, A. F. Izmaylov, J. Bloino, G. Zheng, J. L. Sonnenberg, M. Hada, M. Ehara, K. Toyota, R. Fukuda, J. Hasegawa, M. Ishida, T. Nakajima, Y. Honda, O. Kitao, H. Nakai, T. Vreven, J. A. Montgomery Jr., J. E. Peralta, F. Ogliaro, M. J. Bearpark, J. Heyd, E. N. Brothers, K. N. Kudin, V. N. Staroverov, R. Kobayashi, J. Normand, K. Raghavachari, A. P. Rendell, J. C. Burant, S. S. Iyengar, J. Tomasi, M. Cossi, N. Rega, N. J. Millam, M. Klene, J. E. Knox, J. B. Cross, V. Bakken, C. Adamo, J. Jaramillo, R. Gomperts, R. E. Stratmann, O. Yazyev, A. J. Austin, R. Cammi, C. Pomelli, J. W. Ochterski, R. L. Martin, K. Morokuma, V. G. Zakrzewski, G. A. Voth, P. Salvador, J. J. Dannenberg, S. Dapprich, A. D. Daniels, Ö. Farkas, J. B. Foresman, J. V. Ortiz, J. Cioslowski and D. J. Fox, *Journal*, 2009.
23. Y. Zhao, N. E. Schultz and D. G. Truhlar, *Journal of Chemical Theory and Computation*, 2006, **2**, 364-382.
24. A. V. Marenich, C. J. Cramer and D. G. Truhlar, *Journal of Physical Chemistry B*, 2009, **113**, 6378-6396.
25. A. Golius, L. Gorb, A. Michalkova Scott, F. C. Hill and J. Leszczynski, *Structural Chemistry*, 2015, **26**, 1281-1286.
26. C. Caicedo, C. Iuga, R. Castañeda-Arriaga and J. R. Alvarez-Idaboy, *RSC Advances*, 2014, **4**, 38918-38930.
27. R. Liu, J. Zhang, X. Sun, C. Huang and B. Chen, *Computational and Theoretical Chemistry*, 2014, **1027**, 5-10.
28. R. Álvarez-Diduk, M. T. Ramírez-Silva, A. Galano and A. Merkoçi, *Journal of Physical Chemistry B*, 2013, **117**, 12347-12359.
29. T. R. Heera and L. Cindrella, *Journal of Molecular Modeling*, 2010, **16**, 523-533.
30. S. Corona-Avendaño, G. Alarcón-Angeles, G. A. Rosquete-Pina, A. Rojas-Hernández, A. Gutierrez, M. T. Ramírez-Silva, M. Romero-Romo and M. Palomar-Pardavé, *Journal of Physical Chemistry B*, 2007, **111**, 1640-1647.
31. J. Ho and M. L. Coote, *Theor. Chem. Acc.*, 2010, **125**, 3-21.
32. A. M. Rebollar-Zepeda, T. Campos-Hernández, M. T. Ramírez-Silva, A. Rojas-Hernández and A. Galano, *Journal of Chemical Theory and Computation*, 2011, **7**, 2528-2538.
33. M. Cordova-Gomez, A. Galano and J. R. Alvarez-Idaboy, *RSC Advances*, 2013, **3**, 20209-20218.
34. A. Galano, J. R. Alvarez-Idaboy and M. Francisco-Márquez, *Journal of Physical Chemistry B*, 2011, **115**, 13101-13109.
35. R. Casasnovas, J. Ortega-Castro, J. Donoso, J. Frau and F. Muñoz, *Physical Chemistry Chemical Physics*, 2013, **15**, 16303-16313.
36. J. Ho and M. L. Coote, *Theoretical Chemistry Accounts*, 2010, **125**, 3-21.
37. R. Casasnovas, J. Ortega-Castro, J. Frau, J. Donoso and F. Muñoz, *International Journal of Quantum Chemistry*, 2014, **114**, 1350-1363.
38. D. M. Camaioni and C. A. Schwerdtfeger, *Journal of Physical Chemistry A*, 2005, **109**, 10795-10797.
39. T. Matsui, T. Baba, K. Kamiya and Y. Shigeta, *Physical Chemistry Chemical Physics*, 2012, **14**, 4181-4187.

40. T. Baba, T. Matsui, K. Kamiya, M. Nakano and Y. Shigeta, *International Journal of Quantum Chemistry*, 2014, **114**, 1128-1134.
41. S. Zhang, J. Baker and P. Pulay, *Journal of Physical Chemistry A*, 2010, **114**, 425-431.
42. S. Zhang, J. Baker and P. Pulay, *Journal of Physical Chemistry A*, 2010, **114**, 432-442.
43. S. Zhang, *Journal of Computational Chemistry*, 2012, **33**, 517-526.
44. S. Zhang, *Journal of Computational Chemistry*, 2012, **33**, 2469-2482.
45. T. Matsui, A. Oshiyama and Y. Shigeta, *Chemical Physics Letters*, 2011, **502**, 248-252.

Graphical Abstract

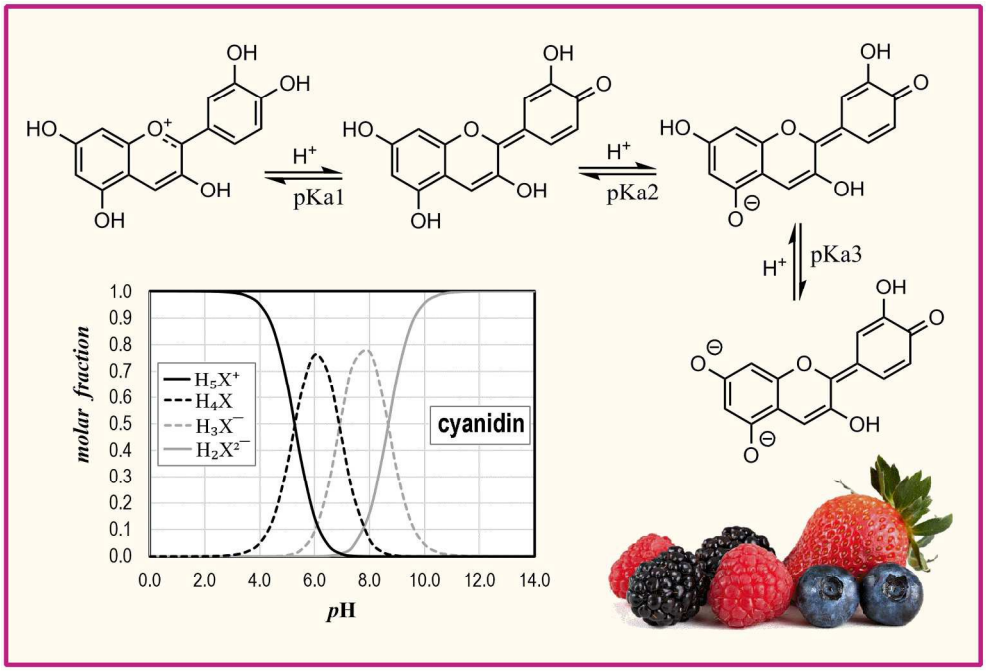

The most likely deprotonation route of 12 anthocyanidins was elucidated, their pK_as are calculated and use to estimate the populations of the different species depending on the *p*H.